Discrete solitons dynamics in $\mathscr{PT}$-symmetric oligomers with complex-valued couplings

O. B. Kirikchi · **N. Karjanto**

Updated January 30, 2021.

Abstract We consider an array of double oligomers in an optical waveguide device. A mathematical model for the system is the coupled discrete nonlinear Schrödinger (NLS) equations, where the gain-and-loss parameter contributes to the complex-valued linear coupling. The array caters to an optical simulation of the parity-time ($\mathscr{PT}$)-symmetry property between the coupled arms. The system admits fundamental bright discrete soliton solutions. We investigate their existence and spectral stability using perturbation theory analysis. These analytical findings are verified further numerically using the Newton-Raphson method and a standard eigenvalue-problem solver. Our study focuses on two natural discrete modes of the solitons: single- and double-excited-sites, also known as onsite and intersite modes, respectively. Each of these modes acquires three distinct configurations between the dimer arms, i.e., symmetric, asymmetric, and antisymmetric. Although both intersite and onsite discrete solitons are generally unstable, the latter can be stable, depending on the combined values of the propagation constant, horizontal linear coupling coefficient, and gain-loss parameter.

Keywords Dimer and oligomer · $\mathscr{PT}$-symmetry · Discrete NLS equation · Bright soliton · Onsite and intersite modes · Dimer arm configuration

PACS 42.65.Hw · 42.65.-k · 42.65.Jx · 05.45.Yv · 45 · 11.30.Er · 45.10.Hj

O. B. Kirikchi
Department of Computing, Goldsmiths, University of London, New Cross, London SE14 6AD, United Kingdom and
Department of Mathematical Sciences, University of Essex, Wivenhoe Park, Colchester, Essex CO4 3SQ, United Kingdom

N. Karjanto
Department of Mathematics, University College, Natural Science Campus, Sungkyunkwan University, 2066 Seobu-ro, Jangan-gu, Suwon 16419, Gyeonggi-do, Republic of Korea
E-mail: natanael@skku.edu

Mathematics Subject Classification (2010) 74J30 · 75J35 · 78A40 · 78A60 · 78M35 · 35Q55 · 37K40 · 37K45 · 35C08

1 Introduction

Dissipative media featuring the parity-time ($\mathscr{PT}$)-symmetry has drawn a great deal of attention ever since Carl Bender and his collaborators proposed the system during the late 1990s [1–4]. The condition for a system of nonlinear evolution equations to be $\mathscr{PT}$-symmetry is that it is invariant with respect to both parity $\mathscr{P}$ and time-reversal $\mathscr{T}$ transformations. This type of symmetry is fascinating since it forms a specific family of non-Hermitian Hamiltonians in quantum physics that will possess a real-valued spectrum until a fixed parameter value of its corresponding complex potential. Above this critical value, the system then belongs to the broken $\mathscr{PT}$-symmetry phase [4–7].

We assume that observable quantities in quantum mechanics are the eigenvalues of operators representing the dynamics of those quantities. Consequently, the eigenvalues, which epitomize the energy spectra, should be real-valued and acquire a lower bound to guarantee that the system features a stable lowest-energy state. To appease this requirement, we contemplate that the operators must be Hermitian. Non-Hermitian Hamiltonians are generally associated with complex-valued eigenvalues and thus degenerate the quantities. Interestingly, it turns out that the Hermiticity is not necessarily required by a Hamiltonian system to satisfy the Postulates of Quantum Mechanics [5]. A necessary condition for a Hamiltonian to be $\mathscr{PT}$-symmetric is that its potential $V(x)$ should satisfy the condition $V(x) = V^*(-x)$ [8].

Although $\mathscr{PT}$-symmetry associates nicely with the standard (local) continuous and discrete nonlinear Schrödinger (NLS) equations as the governing models, it also enjoys an appropriate amalgamation with other nonlinear evolution equations. This includes models with saturable and higher-order nonlinearity [9–16], as well as fractional-order diffraction effect [17–23]. There are also works on nonlocal models that involve $\mathscr{PT}$-symmetry, such as the nonlocal NLS equation [24–28] and nonlocal Davey-Stewartson equations [29–31]. Other models outside the NLS realm where $\mathscr{PT}$-symmetry plays a role include a nonlocal nonlinear Hirota equation [32], a nonlocal long-wave–short wave interaction equation [33], double-ring optical power resonator [34], quantum master Lindblad equation [35], and dampled harmonic Liénard oscillator equations [36].

The term "oligomer" is more well-known in the field of chemistry and comes from the Greek prefix *oligo-*, "a few" and suffix *-mer*, "parts". In this paper, it refers to a repeating structure composed of electronic oscillators or optical waveguides. A dimer is an oligomer system of two coupled oscillators, and it forms the most basic configuration of a system with a $\mathscr{PT}$-symmetry property. Jørgensen and colleagues are the first authors who studied dimer and discussed the conditions for its integrability acquiring a Hamiltonian structure [37, 38]. The dynamics of eigenmodes in other oligomers exhibit large stability areas in both trimer and pentamer systems but a tiny region for tetramers [39].

A distinctive feature of the $\mathscr{PT}$-symmetry system is one part of the dimer loses energy due to a damping effect while another oscillator gains energy from an external source. Indeed, the idea of $\mathscr{PT}$-symmetry was accomplished experimentally for the first time on dimers consisting of two coupled optical waveguides [40, 41]. Optical analogs using two coupled waveguides with gain and loss were investigated in [42–44], where such couplers have been considered previously in the 1990s [37, 38, 45].

$\mathscr{PT}$-symmetric analogs in coupled oscillators have also been proposed theoretically and experimentally [46–49]. A $\mathscr{PT}$-symmetric system of coupled oscillators with gain and loss can form a Hamiltonian system and exhibits a twofold transition which depends on the size of the coupling parameter [50–52]. A comparison between analytical study and numerical approach in a $\mathscr{PT}$-system with periodically varying-in-time gain and loss modeled by two coupled Schrödinger equations shows a remarkable agreement [53]. Besides showing that the problem can be reduced to a perturbed pendulum-like equation, they also investigated an approximate threshold for the broken $\mathscr{PT}$-symmetry phase, cf. [54].

In the case of the anticontinuum limit, breathers are common occurrences in the $\mathscr{PT}$-symmetric chain of dimers. Particularly, a system of amplitude equations governing the breather envelope remains conservative and the small-amplitude $\mathscr{PT}$-breathers are stable for a finite time scale [55]. There exists a fascinating class of optical systems where a coupling or interaction causes the systems to be $\mathscr{PT}$-symmetric. Additionally, symmetry-breaking bifurcations in specific reciprocal and nonreciprocal $\mathscr{PT}$-symmetric systems have a promising application in optical isolators and diodes [56], cf. [14, 15, 21, 40, 57].

In addition to the $\mathscr{PT}$-symmetry phase transition, the reciprocal transmission and unidirectional reflectionless features are appealing to many. The axial and reflection $\mathscr{PT}$-symmetry lead to symmetric reflection and symmetric transmission, respectively [58]. Two interesting nonreciprocal phenomena are unidirectional lightwave propagation and unidirectional lasing, where both are independent of the input direction. When they are combined in a $\mathscr{PT}$-symmetric setting, the unidirectional destructive interference plays an important role in wave dynamics due to the vanishing of spectral singularity [59].

In particular, we are interested in the nonlinear dynamics of $\mathscr{PT}$-symmetric chain of dimers that can be modeled by the discrete nonlinear Schrödinger (DNLS) type of equations due to its abundance applications in nonlinear optics and Bose-Einstein condensates (BEC) [60–62]. Transport on dimers with $\mathscr{PT}$-symmetric potentials are modeled by the coupled DNLS equations with gain and loss, which was relevant among others to experiments in optical couplers and proposals on BEC in $\mathscr{PT}$-symmetric double-well potentials [63]. This proposed model is integrable and its integrability is further utilized to build up the phase portrait of the system. The existence and stability of localized mode solutions to nonlinear dynamical lattices of the DNLS type of equations with two-component settings have been considered and a general framework has been provided in [64]. A dual-core nonlinear waveguide with the $\mathscr{PT}$-symmetry has been expanded by including a periodic sinusoidal variation of the loss-gain coefficients and synchronous variation of the inter-core coupling constant [65]. The system leads to multiple-collision interactions among stable solitons. A study of the nonlinear nonreciprocal dimer in an anti-Hermitian lattice with cubic nonlinearity has been explored recently [66].

In our previous work, we have considered the existence and linear stability of fundamental bright discrete solitons in $\mathscr{PT}$-symmetric dimers with gain-loss terms [67], in a chain of charge-parity ($\mathscr{CP}$)-symmetric dimers [68], and in a chain of $\mathscr{PT}$-symmetric dimers with cubic-quintic nonlinearity [69]. The latter covers the snaking behavior in the bifurcation diagrams for the existence of standing localized solutions. In this paper, we consider the coupled discrete linear and nonlinear Schrödinger equations on oligomers with complex couplings as systems of $\mathscr{PT}$-symmetric potentials. This proposed model arises as nonlinear optical waveguide couplers or a BEC emulation in double-well potentials with $\mathscr{PT}$-symmetry and we hope to stimulate a series of experiments along this direction.

This article is organized as follows. We introduce the corresponding equations modeling the dynamics of the $\mathscr{PT}$-symmetric chain of dimers in Section 2. We investigate the existence of fundamental discrete solitons for a small value of the linear horizontal coupling between two adjacent sites using the theory of perturbation. We analyze the stability of the fundamental discrete solitons by solving the corresponding eigenvalue problems in Section 3. Since the expression of the corresponding eigenvectors from the linearized eigenvalue problem is arduous, we also employ perturbation expansion with respect to the gain-loss parameter, which also assumed to be small. Section 4 compares analytical findings with numerical calculations. We display the plots of the spectra and typical dynamics of discrete solitons for different parameter values. Section 5 concludes our study.

2 Mathematical model

The coupled discrete NLS equations that govern the dynamics of $\mathscr{PT}$-symmetric chains of dimers are given as follows:

$$\begin{aligned}\dot{u}_n &= i|u_n|^2u_n + i\varepsilon\Delta_2 u_n + \gamma v_n + iv_n,\\ \dot{v}_n &= i|v_n|^2v_n + i\varepsilon\Delta_2 v_n - \gamma u_n + iu_n,\end{aligned} \tag{1}$$

where the dots represent the derivative with respect to the evolution variable, which is the physical time t for BEC and the propagation direction z in the case of nonlinear optics. Both $u_n = u_n(t)$ and $v_n = v_n(t)$ are complex-valued wave functions at the site $n \in \mathbb{Z}$. The coefficient $0 < \varepsilon << 1$ acts as the linear horizontal coupling constant between two adjacent sites. The quantities following ε are the discrete Laplacian factors in one spatial dimension, explicitly given as $\Delta_2 u_n = (u_{n+1} - 2u_n + u_{n-1})$ and $\Delta_2 v_n = (v_{n+1} - 2v_n + v_{n-1})$. The coefficient γ represents the gain and loss factor and contributes to the complex-valued coupling of the system. Without loss of generality, we will take $\gamma > 0$. We only consider the solitons solutions that satisfy the localization conditions, i.e., $u_n, v_n \to 0$ as $n \to \pm\infty$.

The current model employs complex-valued coefficients in the vertical coupling between the parallel arrays, while the previous work [67] and [68] adopted purely imaginary and real-valued vertical coupling between the parallel arrays, respectively, which acts as the gain or loss in the system. Additionally, they also included the real-valued and purely imaginary phase-velocity mismatch between the horizontal cores in [67] and [68], respectively, which is absent in our current model.

For the uncoupled case, also known as the anticontinuum limit, i.e., when $\varepsilon = 0$, the governing equations (1) reduce to another $\mathscr{PT}$-symmetric system in the presence of complex-valued coupling but in the absence of discrete Laplacian terms, which has been investigated in [56]. A similar setup to our model was studied in [70] where the authors approached from a dynamical system point of view by incorporating the so-called Stokes variables into the system.

We substitute the following expressions for the complex-valued wave functions u_n and v_n to obtain static solutions of the governing equations (1):

$$u_n = A_n e^{i\omega t}, \qquad v_n = B_n e^{i\omega t}, \tag{2}$$

where the coefficients $A_n, B_n \in \mathbb{C}$, and $\omega \in \mathbb{R}$ is the propagation constant. We obtain the following static equations for the $\mathscr{PT}$-symmetry dimer:

$$\begin{aligned}\omega A_n &= |A_n|^2 A_n + \varepsilon(A_{n+1} - 2A_n + A_{n-1}) - i\gamma B_n + B_n,\\ \omega B_n &= |B_n|^2 B_n + \varepsilon(B_{n+1} - 2B_n + B_{n-1}) + i\gamma A_n + A_n.\end{aligned} \tag{3}$$

The static equations (3) for $\varepsilon = 0$ has been analyzed in details in [37,38,56]. For sufficiently small but nonzero linear horizontal coupling ε, one can verify the existence of soliton solutions emerging from the anticontinuum limit by employing a generalization of the Implicit Function Theorem to a Banach space [71,72]. We can adopt the existence analysis of [63] to our system rather straightforwardly. In this paper, we only derive the asymptotic series of the soliton solutions and do not proceed to the theorem in more detail.

We express the complex-valued quantities A_n and B_n as perturbation expansions in terms of the small linear horizontal coupling ε:

$$\begin{aligned}A_n &= A_n^{(0)} + \varepsilon A_n^{(1)} + \varepsilon^2 A_n^{(2)} + \dots,\\ B_n &= B_n^{(0)} + \varepsilon B_n^{(1)} + \varepsilon^2 B_n^{(2)} + \dots.\end{aligned} \tag{4}$$

We substitute these expansions (4) to the static equations (3) and collect the terms in successive powers of ε. We then obtain the following equations at $\mathscr{O}(1)$ and $\mathscr{O}(\varepsilon)$, respectively:

$$\begin{aligned}A_n^{(0)}(1+i\gamma) &= B_n^{(0)}(\omega - B_n^{(0)} B_n^{*(0)}),\\ B_n^{(0)}(1-i\gamma) &= A_n^{(0)}(\omega - A_n^{(0)} A_n^{*(0)}).\end{aligned} \tag{5}$$

and

$$\begin{aligned}A_n^{(1)}(1+i\gamma) &= B_n^{(1)}(\omega - 2B_n^{(0)} B_n^{*(0)}) - {B_n^{(0)}}^2 B_n^{*(1)} - \Delta_2 B_n^{(0)},\\ B_n^{(1)}(1-i\gamma) &= A_n^{(1)}(\omega - 2A_n^{(0)} A_n^{*(0)}) - {A_n^{(0)}}^2 A_n^{*(1)} - \Delta_2 A_n^{(0)}.\end{aligned} \tag{6}$$

The corresponding bright discrete soliton solutions admit two natural, fundamental modes for any $\varepsilon > 0$, which range from the anticontinuum to anticontinuum limits. They are the one-excited- and two-excited-sites, also known as the onsite and intersite bright discrete modes, respectively. The remainder of our discussion will focus on these two natural fundamental modes.

2.1 Dimers

In the anticontinuum limit $\varepsilon \to 0$, the time-independent solution of (3), i.e., (5), can be written as $A_n^{(0)} = \tilde{a}_0 e^{i\phi_a}$ and $B_n^{(0)} = \tilde{b}_0 e^{i\phi_b}$, where both amplitudes are positive real valued, i.e., $\tilde{a}_0 > 0$ and $\tilde{b}_0 > 0$. Solving the resulting polynomial equations for $\tilde{a}_0$ and $\tilde{b}_0$ will yield [56]

$$\tilde{a}_0 = \tilde{b}_0 = 0, \tag{7}$$

$$\tilde{a}_0 = \tilde{b}_0 = \sqrt{\omega - \sqrt{1+\gamma^2}}, \tag{8}$$

$$\tilde{a}_0 = -\tilde{b}_0 = \sqrt{\omega + \sqrt{1+\gamma^2}}, \tag{9}$$

$$\begin{aligned} \tilde{a}_0 &= \frac{1}{\sqrt{2}}\sqrt{\omega + \sqrt{\omega^2 - 4(1+\gamma^2)}}, \\ \tilde{b}_0 &= \frac{1}{2}\frac{\sqrt{\omega + \sqrt{\omega^2 - 4(1+\gamma^2)}}\left[\omega - \sqrt{\omega^2 - 4(1+\gamma^2)}\right]}{\sqrt{2(1+\gamma^2)}}, \end{aligned} \tag{10}$$

and the phase $\phi_b - \phi_a = \arctan\gamma$. Due to the gauge invariance in the phase of the $\mathscr{PT}$-symmetry system (1), we can set $\phi_a = 0$ without loss of generality. Thus, $\phi_b = \arctan(\gamma)$. Solutions (8), (9), and (10) are referred to as the symmetric, antisymmetric, and asymmetric solutions, respectively. The asymmetric solution (10) emanates from a pitchfork bifurcation from the symmetric solution (8) at $\omega = 2\sqrt{1+\gamma^2}$.

Another variant of interesting dimers where the coupling between the oscillators provide gain to the system was considered in [68,73,74]. Such a system may model the propagation of electromagnetic waves in coupled waveguides embedded in an active medium. The dimer considered herein when $\varepsilon \to 0$ is different as in our case the coupling between the cores does not only provide gain but also loss.

2.2 Intersite discrete solitons

The mode structure of the intersite discrete solitons in the anticontinuum limit is given by

$$\begin{aligned} A_n^{(0)} &= \begin{cases} \tilde{a}_0 & n = 0,1, \\ 0 & \text{otherwise}, \end{cases} \\ B_n^{(0)} &= \begin{cases} \tilde{b}_0 e^{i\phi_b} & n = 0,1, \\ 0 & \text{otherwise}. \end{cases} \end{aligned} \tag{11}$$

For $\varepsilon \neq 0$, we can write the first-order correction coefficients as $A_n^{(1)} = \tilde{a}_1$ and $B_n^{(1)} = \tilde{b}_1 e^{i\phi_b}$. Substituting these to the $\mathscr{O}(\varepsilon)$ equations (6) gives the following expressions for $\tilde{a}_1$ and $\tilde{b}_1$:

$$\begin{aligned} \tilde{a}_1 &= \frac{\tilde{b}_1(\omega - 3\tilde{b}_0^2) + \tilde{b}_0}{\sqrt{1+\gamma^2}}, \\ \tilde{b}_1 &= \frac{\tilde{a}_1(\omega - 3\tilde{a}_0^2) + \tilde{a}_0}{\sqrt{1+\gamma^2}}. \end{aligned} \tag{12}$$

Equations (11) and (12) give the asymptotic expansions for A_n and B_n up to the first-order correction for the intersite discrete solitons. Higher-order corrections can be calculated by continuing a similar procedure. Since the first two terms are sufficient for our analysis, we exclude those higher-order terms.

2.3 Onsite discrete solitons

The onsite discrete soliton in the anticontinuum limit admits the following mode structure:

$$\begin{aligned} A_n^{(0)} &= \begin{cases} \tilde{a}_0 & n = 0, \\ 0 & \text{otherwise}, \end{cases} \\ B_n^{(0)} &= \begin{cases} \tilde{b}_0 e^{i\phi_b} & n = 0, \\ 0 & \text{otherwise}. \end{cases} \end{aligned} \tag{13}$$

Employing a similar calculation as in the intersite case, we acquire the following expressions for $\tilde{a}_1$ and $\tilde{b}_1$ corresponding to $\mathscr{O}(\varepsilon)$ corrections derived from equations (6):

$$\begin{aligned} \tilde{a}_1 &= \frac{\tilde{b}_1(\omega - 3\tilde{b}_0^2) + 2\tilde{b}_0}{\sqrt{1+\gamma^2}}, \\ \tilde{b}_1 &= \frac{\tilde{a}_1(\omega - 3\tilde{a}_0^2) + 2\tilde{a}_0}{\sqrt{1+\gamma^2}}. \end{aligned} \tag{14}$$

The asymptotic expansions for A_n and B_n up to the first-order correction for the onsite discrete solitons are thus given by expressions (13) and (14). Likewise, higher-order corrections can be obtained using a similar calculation. We also exclude higher-order terms for this case.

3 Stability analysis

In the following, we consider six configurations, which are combinations of the intersite and onsite discrete solitons with the three solutions of the dimers (8)–(10). We will denote them by subscripts (i) and (o) for intersite and onsite discrete solitons, and (s), (at), and (as) for the symmetric, antisymmetric, and asymmetric types of solution, respectively.

We analyze the linear stability of the discrete soliton solutions by solving the corresponding eigenvalue problem. We propose a linearization ansatz for the complex-valued functions u_n and v_n with $|\widetilde{\varepsilon}| \ll 1$, written as follows:

$$\begin{aligned} u_n &= (A_n + \widetilde{\varepsilon}(K_n + iL_n)e^{\lambda t})e^{i\omega t} \\ v_n &= (B_n + \widetilde{\varepsilon}(P_n + iQ_n)e^{\lambda t})e^{i\omega t}. \end{aligned}$$

Substituting these expressions to the governing equations (1), we obtain the linearized equation at $\mathscr{O}(\tilde{\varepsilon})$:

$$\begin{aligned}\lambda K_n &= -(A_n^2-\omega)L_n - \varepsilon(L_{n+1}-2L_n+L_{n-1}) + \gamma P_n - Q_n,\\ \lambda L_n &= (3A_n^2-\omega)K_n + \varepsilon(K_{n+1}-2K_n+K_{n-1}) + \gamma Q_n + P_n,\\ \lambda P_n &= -\left[\mathrm{Re}^2(B_n)+3\,\mathrm{Im}^2(B_n)-\omega\right]Q_n - \gamma K_n - L_n\\ &\quad -\varepsilon(Q_{n+1}-2Q_n+Q_{n-1}) - 2\,\mathrm{Re}(B_n)\,\mathrm{Im}(B_n)P_n,\\ \lambda Q_n &= \left[3\,\mathrm{Re}^2(B_n)+\mathrm{Im}^2(B_n)-\omega\right]P_n - \gamma L_n + K_n\\ &\quad +\varepsilon(P_{n+1}-2P_n+P_{n-1}) + 2\,\mathrm{Re}(B_n)\,\mathrm{Im}(B_n)Q_n,\end{aligned} \tag{15}$$

which need to be solved for the eigenvalue (or, spectrum) λ and the corresponding eigenvector

$$[\{K_n\},\{L_n\},\{P_n\},\{Q_n\}]^T.$$

The solution u_n is said to be (linearly) stable when $\mathrm{Re}(\lambda)\le 0$ for all the spectra $\lambda\in\mathbb{C}$ and unstable otherwise. However, as the spectra will come in pairs, a solution is therefore neutrally stable when $\mathrm{Re}(\lambda)=0$ for all $\lambda\in\mathbb{C}$.

3.1 Continuous spectrum

The eigenvalues of (15) consist of both continuous and discrete spectra. In this subsection, we investigate the former by considering the limit $n\to\pm\infty$. We introduce the following plane-wave ansatz to the eigenvector components: $K_n=\hat{k}e^{ikn}$, $L_n=\hat{l}e^{ikn}$, $P_n=\hat{p}e^{ikn}$, and $Q_n=\hat{q}e^{ikn}$, where $k\in\mathbb{R}$. Substituting these ansatzes to (15), we obtain the following system of linear equations written in matrix form:

$$\lambda\begin{bmatrix}\hat{k}\\ \hat{l}\\ \hat{p}\\ \hat{q}\end{bmatrix} = \begin{bmatrix}0 & \xi & \gamma & -1\\ -\xi & 0 & 1 & \gamma\\ -\gamma & -1 & 0 & \xi\\ 1 & -\gamma & -\xi & 0\end{bmatrix}\begin{bmatrix}\hat{k}\\ \hat{l}\\ \hat{p}\\ \hat{q}\end{bmatrix} \tag{16}$$

where $\xi=\omega-2\varepsilon(\cos k-1)$. This matrix equation (16) can be solved analytically to yield the following linear dispersion relationship:

$$\lambda^2 = -(1+\gamma^2)-\xi^2\pm 2|\xi|\sqrt{1+\gamma^2}. \tag{17}$$

Thus, the ranges for the continuous spectrum are given by $\lambda\in\pm[\lambda_{1-},\lambda_{2-}]$ and $\lambda\in\pm[\lambda_{1+},\lambda_{2+}]$, where the spectrum boundaries $\lambda_{1\pm}$ and $\lambda_{2\pm}$ lie on the imaginary axis:

$$\lambda_{1\pm} = \pm i\sqrt{1+\gamma^2+\omega^2\mp 2|\omega|\sqrt{1+\gamma^2}}, \tag{18}$$

$$\lambda_{2\pm} = \pm i\sqrt{1+\gamma^2+(\omega+4\varepsilon)^2\mp 2|\omega+4\varepsilon|\sqrt{1+\gamma^2}}. \tag{19}$$

We can attain these expressions (18) and (19) by substituting $k=0$ and $k=\pi$ to the linear dispersion relationship (17), respectively.

3.2 Discrete spectrum

In this subsection, we seek discrete spectra of the linear eigenvalue problem (15) using a similar asymptotic expansion implemented in Section 2, albeit with weak linear horizontal coupling ε. Let the expansion read

$$X = X^{(0)}+\sqrt{\varepsilon}X^{(1)}+\varepsilon X^{(2)}+\dots, \tag{20}$$

where $X=\{\lambda,K_n,L_n,P_n,Q_n\}$. Then, substituting the expansion (20) to the linear eigenvalue problem (15), we obtain other sets of linear equations according to the successive order of ε: $\mathscr{O}(1)$, $\mathscr{O}(\sqrt{\varepsilon})$, $\mathscr{O}(\varepsilon)$, etc.

At the lowest order, we attain the corresponding stability equation for the $\mathscr{PT}$-symmetric chain of dimers, in which for general values of γ it has been elaborated in [56]. Although the resulting eigenvalues have relatively simple expressions, the corresponding eigenvectors are cumbersome, which are rather worthless for further scrutiny in correcting higher-order eigenvalues. We then restraint our analysis for the case of small gain-loss parameter γ and expand the variables (20) in γ for each expression at $\mathscr{O}(\varepsilon^{n/2})$, $n\in\mathbb{N}_0$, obtained from (15). We write the following:

$$X^{(j)} = X^{(j,0)}+\gamma X^{(j,1)}+\gamma^2X^{(j,2)}+\dots,$$

where $j=0,1,2,\dots$. These two small parameters ε and γ are independent of each other. The steps for calculating eigenvalues $\lambda^{(j,k)}$, $j,k\in\mathbb{N}_0$ have been outlined in detail in the Appendix of [67]. Here, we will present the results instantaneously.

3.2.1 Intersite discrete soliton

Instead of two types of intersite discrete solitons that emerged from the analysis in [67], i.e., symmetric and antisymmetric, we obtain an additional type, i.e., asymmetric one. All of them have in general one pair of eigenvalues that bifurcate from the origin for small ε and two pairs of nonzero eigenvalues. They are asymptotically given by

$$\lambda_{(\mathrm{i,s})} = \sqrt{\varepsilon}\left(2\sqrt{\omega-1}-\gamma^2/(2\sqrt{\omega-1})+\dots\right)+\mathscr{O}(\varepsilon), \tag{21}$$

$$\lambda_{(\mathrm{i,at})} = \sqrt{\varepsilon}\left(2\sqrt{\omega+1}+\gamma^2/(2\sqrt{\omega+1})+\dots\right)+\mathscr{O}(\varepsilon), \tag{22}$$

$$\lambda_{(\mathrm{i,as})} = \sqrt{\varepsilon}\left(2\sqrt{\omega}+\dots\right)+\mathscr{O}(\varepsilon), \tag{23}$$

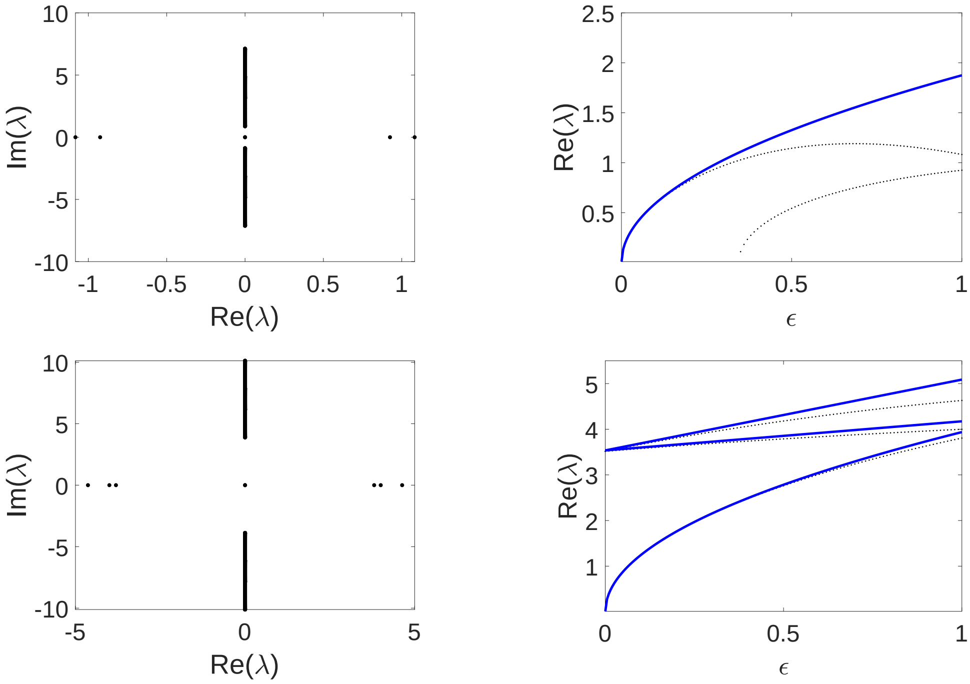

Fig. 1 The spectra of unstable symmetric intersite discrete solitons with $\omega = 2$, $\gamma = 0.5$ (top panels) and $\omega = 5$, $\gamma = 0.9$ (bottom panels). The left panels feature the spectrum characteristics in the complex plane for $\varepsilon = 1$. The right panels present the real-part of the spectrum as a function of the linear horizontal coupling constant ε. The solid blue curves are the asymptotic approximations presented in Subsubsection 3.2.1 while the dots are obtained from a numerical calculation.

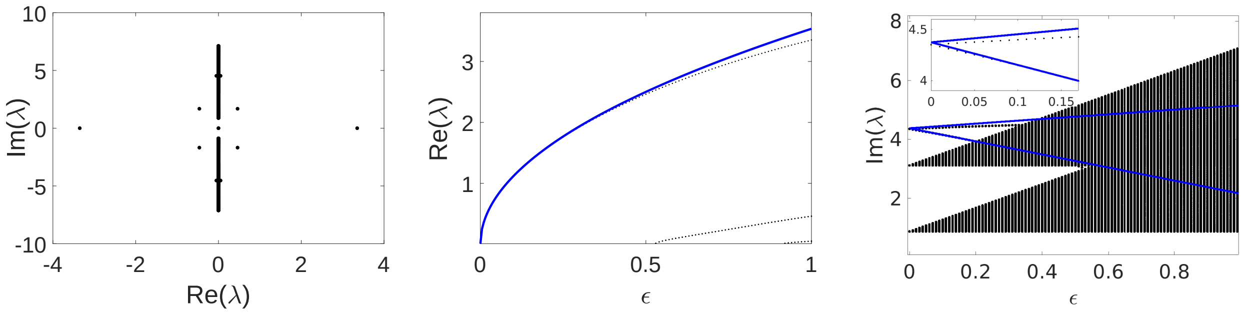

(a) (b) (c)

Fig. 2 The spectra of unstable antisymmetric intersite discrete solitons with $\omega = 2$ and $\gamma = 0.5$. Panel (a) displays the spectra in the complex plane for $\varepsilon = 1$. Panels (b) and (c) present the real-part and imaginary-part of the spectrum λ as a function of the horizontal linear coupling constant ε, respectively. The solid blue and dotted curves are attained from the asymptotic approximation and numerical calculation, respectively.

for the eigenvalues bifurcating from the origin and

$$\lambda_{(\mathrm{i,s})} = \begin{cases} \left(2\sqrt{\omega-2} + \gamma^2 \frac{\omega-4}{2\sqrt{\omega-2}} + \dots\right) \\ +\varepsilon\left(\sqrt{\omega-2} - \gamma^2 \frac{\omega}{4\sqrt{\omega-2}} + \dots\right) + \mathscr{O}\left(\varepsilon^{3/2}\right), \\ \left(2\sqrt{\omega-2} + \gamma^2 \frac{\omega-4}{2\sqrt{\omega-2}} + \dots\right) \\ +\varepsilon\left(\frac{1}{\sqrt{\omega-2}} + \gamma^2 \frac{\omega}{4(\omega-2)^{3/2}} + \dots\right) + \mathscr{O}\left(\varepsilon^{3/2}\right), \end{cases} \tag{24}$$

$$\lambda_{(\mathrm{i,at})} = \begin{cases} \left(2i\sqrt{\omega+2} + \gamma^2 \frac{i(\omega+4)}{2\sqrt{\omega+2}} + \dots\right) \\ -\varepsilon\left(i\sqrt{\omega+2} + \gamma^2 \frac{3i(\omega^2+5\omega+4)}{8(\omega+2)^{3/2}} + \dots\right) + \mathscr{O}\left(\varepsilon^{3/2}\right), \\ \left(2i\sqrt{\omega+2} + \gamma^2 \frac{i(\omega+4)}{2\sqrt{\omega+2}} + \dots\right) \\ +\varepsilon\left(\frac{i}{\sqrt{\omega+2}} + \gamma^2 \frac{i(5\omega^2+21\omega+12)}{8(\omega+2)^{3/2}} + \dots\right) + \mathscr{O}\left(\varepsilon^{3/2}\right), \end{cases} \tag{25}$$

$$\lambda_{(\mathrm{i,as})} = \begin{cases} \left(\sqrt{4-\omega^2} - \gamma^2 \frac{2i}{\sqrt{\omega^2-4}} + \dots\right) \\ +\varepsilon\left(\frac{3i\omega}{\sqrt{\omega^2-4}} + \gamma^2 \frac{6i\omega}{(\omega^2-4)^{3/2}} + \dots\right) + \mathscr{O}\left(\varepsilon^{3/2}\right), \\ \left(\sqrt{4-\omega^2} - \gamma^2 \frac{2i}{\sqrt{\omega^2-4}} + \dots\right) \\ +\varepsilon\left(\frac{i\omega}{\sqrt{\omega^2-4}} + \gamma^2 \frac{2i\omega}{(\omega^2-4)^{3/2}} + \dots\right) + \mathscr{O}\left(\varepsilon^{3/2}\right), \end{cases} \tag{26}$$

for the nonzero eigenvalues.

3.2.2 Onsite discrete soliton

Similarly, we also have three types of onsite discrete solitons with each one generally has only one pair of nonzero eigenvalues. For a small value of ε, the symmetric, antisymmetric, and asymmetric onsite discrete solitons are given asymptotically as follows, respectively:

$$\lambda_{(\mathrm{o,s})} = \left(2\sqrt{\omega-2}+\gamma^2\frac{(\omega-4)}{2\sqrt{\omega-2}}+\dots\right) + \varepsilon\left(\frac{2}{\sqrt{\omega-2}}+\gamma^2\frac{\omega}{2(\omega-2)^{3/2}}+\dots\right)+\mathscr{O}\left(\varepsilon^{3/2}\right), \quad (27)$$

$$\lambda_{(\mathrm{o,at})} = \left(2i\sqrt{\omega+2}+\gamma^2\frac{i(\omega+4)}{2\sqrt{\omega+2}}+\dots\right) + \varepsilon\left(\frac{2i}{\sqrt{\omega+2}}+\gamma^2\frac{i\omega}{2(\omega+2)^{3/2}}+\dots\right)+\mathscr{O}\left(\varepsilon^{3/2}\right), \quad (28)$$

$$\lambda_{(\mathrm{o,as})} = \left(i\sqrt{\omega^2-4}-\gamma^2\frac{2i}{\sqrt{\omega^2-4}}+\dots\right) + \varepsilon\left(\frac{2i\omega}{\sqrt{\omega^2-4}}+\gamma^2\frac{4i\omega}{(\omega^2-4)^{3/2}}+\dots\right)+\mathscr{O}\left(\varepsilon^{3/2}\right). \quad (29)$$

4 Numerical results

To solve the static equations numerically, i.e., Eq. (3), we implemented the Newton-Raphson method. After we obtain the numerical soliton solutions, we investigate their stability by solving the corresponding linear eigenvalue problem (15) using a standard eigenvalue problem solver. In this section, we will compare the analytical calculations obtained in the previous sections with the numerical results.

First, we examine the family of symmetric intersite discrete solitons. The left panels of Figure 1 display both continuous and discrete spectra in the complex plane for $\varepsilon = 1$ and the right panels of Figure 1 reveal the dynamics of the real-valued spectrum as a function of the linear horizontal coupling ε. The parameter values for the top panels of Figure 1 are $\omega = 2$ and $\gamma = 0.5$. For these parameter values, there exists only one pair of discrete spectrum in the beginning (anticontinuum limit). As the coupling ε value increases, one of the nonzero spectra that was initially on the imaginary axis becomes real-valued, too.

The bottom panels of Figure 1 demonstrate the spectra for a sufficiently large value of the propagation constant ($\omega = 5$ and $\gamma = 0.9$). We observe that in the anticontinuum limit, one pair of the discrete spectrum is located at the origin while two pairs lie on the real axis. As the linear horizontal coupling ε increases, the pair that was initially at the origin moves closer to the other two pairs. In the right panels, we also illustrate the approximate plot for the discrete spectrum in solid blue curves, where a satisfying agreement is attained for small values of the coupling ε. In all cases, the family of symmetric intersite discrete solitons is unstable in the continuum limit $\varepsilon \to \infty$.

Second, we consider the family of antisymmetric intersite discrete solitons. Figure 2(a) displays a typical distribution of both continuous and discrete spectra in the complex plane for $\varepsilon = 1$, $\omega = 2$ and $\gamma = 0.5$. Figures 2(b) and 2(c) feature the real-part and imaginary-part of the discrete spectrum as a function of the linear horizontal coupling parameter ε, respectively. We notice that there exists a pair of the discrete spectrum that bifurcates from the origin. For this particular value of the propagation constant, the spectra satisfy the condition $\lambda^2 < \lambda_{2-}^2$ in the anticontinuum limit $\varepsilon \to 0$. As the linear horizontal coupling ε increases, the continuous and discrete spectra collide, and consequently, the eigenvalues become complex-valued. Similar to the previous case, the family of antisymmetric intersite discrete solitons is unstable in the continuum limit $\varepsilon \to \infty$ for all the chosen parameter values.

Third, the final case for intersite discrete solitons is the family of asymmetric ones. Figure 3 displays a common spectrum distribution in the complex plane for a particular choice of parameters ω and γ. Although the complex eigenvalues are not visible, the asymmetric intersite discrete solitons yield unstable solutions for the set of calculated parameters in the continuum limit. In the anticontinuum limit, the position of the discrete spectrum for the previous case of the antisymmetric intersite is above all the continuous spectrum, *viz.* Figure 2. The main interesting part is that the unstable eigenvalues bifurcate into the complex plane, i.e., the emergence of eigenvalues with the nonzero imaginary part. For the asymmetric intersite case, the position of the discrete spectrum is in between the continuous one and the imaginary part remains zero.

Figure 4–6 present the spectrum characteristics for the families of onsite discrete solitons. Different from the families of intersite discrete solitons that are consistently unstable, the families of onsite discrete solitons can be stable depending on the parameter values. Figure 4(a) displays the imaginary-part of the discrete spectrum as a function of the linear horizontal coupling coefficient ε for the family of symmetric onsite discrete solitons. The choice of ω, in this case, corresponds to stable discrete solitons. However, there are regions of instability for different parameter values of ω that may depend on γ and ε. Figure 4(b) displays the regions of (in)stability for the symmetric onsite discrete solitons in the (ε, ω)-plane for three distinct values of γ. We observe that the real-part of the contribution of the gain-loss parameter γ toward the $\mathscr{PT}$-symmetric system for this particular case

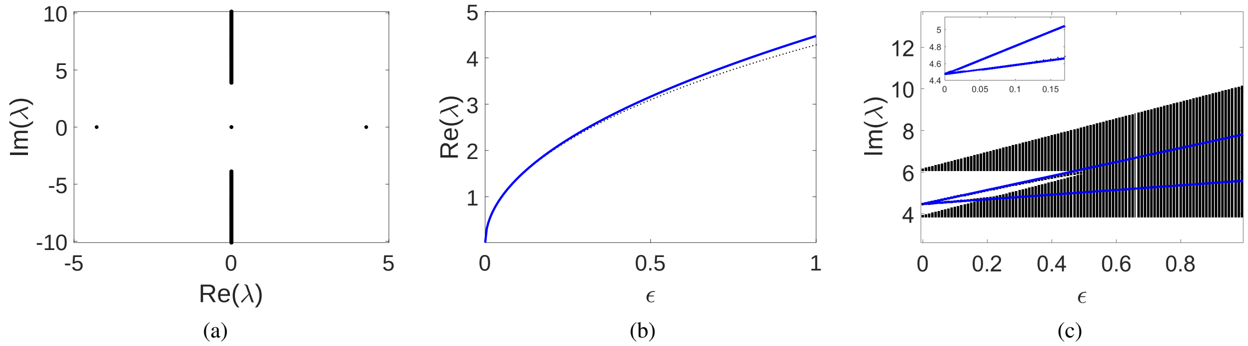

Fig. 3 The spectra of unstable asymmetric intersite discrete solitons with $\omega = 5$ and $\gamma = 0.5$. Panel (a) displays the spectra in the complex plane for $\varepsilon = 1$. Panels (b) and (c) present the eigenvalues λ as a function of the coupling constant ε. The solid blue and dotted curves are attained from the asymptotic approximation and numerical calculation, respectively.

seems to be beneficial since it expands the region of stability for the family of symmetric onsite discrete solitons.

Figure 5 shows a typical feature of the spectrum for the family of antisymmetric onsite discrete solitons. As depicted in Figure 5(a) for $\varepsilon = 1$, due to the presence of quartet complex-valued eigenvalues, this family of solitons is generally unstable. Since the instability occurs due to the collision of the discrete spectrum with the continuous one, stability regions may present before the encounter. Figure 5(c) shows the sectors where the family of antisymmetric onsite discrete solitons is unstable between the curves. These solitons are unstable in the continuum limit $\varepsilon \to \infty$. Figure 6 shows the family of asymmetric onsite discrete solitons that is stable in the region of their existence. Note that this family of solitons bifurcates from the symmetric ones.

Finally, we present in Figures 7–10 the time dynamics of the unstable solutions shown in Figures 1–5. We obtain one feature of typical dynamics in the form of discrete soliton destructions. One may attain oscillating solitons or asymmetric solutions between the arms.

Similar to the families of discrete soliton in a $\mathscr{P}\mathscr{T}$-symmetric chain of dimers with purely imaginary vertical coupling and real-valued velocity mismatch considered in [67], most of the discrete solitons emanating from our model is also unstable, while the soliton families in a chain of dimers with $\mathscr{C}\mathscr{P}$-symmetry considered in [68] are stable. Stable discrete solitons in [67] occur when both the propagation constant and gain-loss parameter are small. On the other hand, the gain-loss coefficient does not influence the width of the snakes for the case $\mathscr{P}\mathscr{T}$-symmetry chain of dimers with cubic-quintic nonlinearity [69].

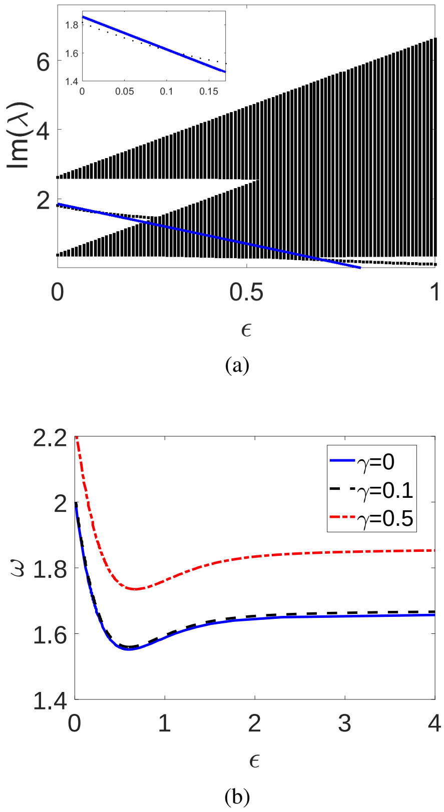

Fig. 4 (a) The imaginary-part of the spectrum as a function of the linear horizontal coupling parameter ε and its approximation of symmetric onsite discrete solitons with $\omega = 1.5$, $\gamma = 0.5$. (b) The stability region of the family of symmetric onsite discrete solitons in the (ε, ω)-plane for three distinct values of γ. The family of symmetric onsite discrete solitons are unstable above the curves.

5 Conclusion

We have presented a model of double oligomers optical waveguide array using the discrete NLS equations with complex-valued coupling. The structure can be implemented in a discrete system with the $\mathscr{P}\mathscr{T}$-symmetry characteristic. Both analytical and numerical results suggest the existence of fundamental bright discrete soliton solutions. We restricted our study to the two discrete modes of the solitons, the

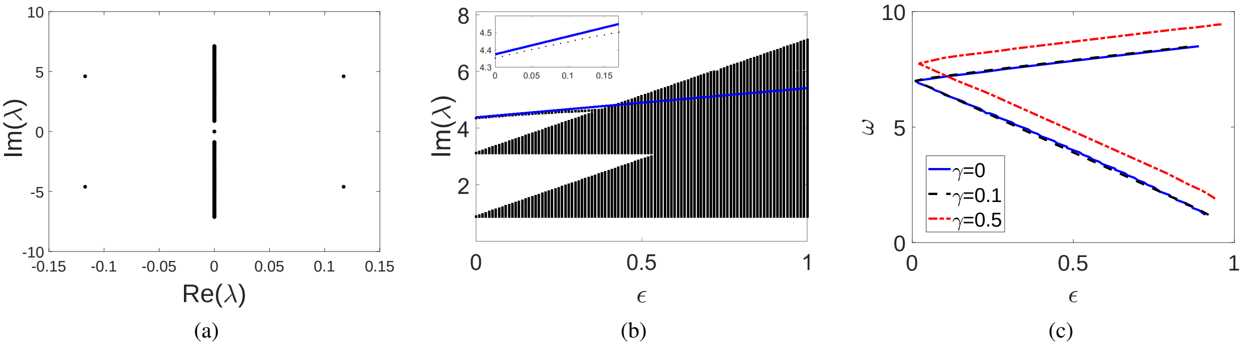

Fig. 5 Panel (a) displays eigenvalues of antisymmetric onsite discrete soliton for $\omega = 2$, $\gamma = 0.5$, and $\varepsilon = 1$. (b) The imaginary-part of the spectrum as a function of the linear horizontal coupling parameter ε. (c) The stability diagram of the discrete solitons for several values of γ. The family of antisymmetric onsite discrete solitons is unstable between the curves.

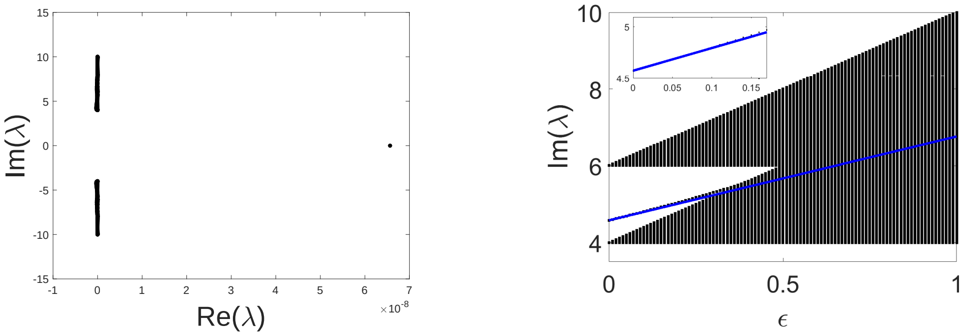

Fig. 6 The left panel displays the eigenvalues of asymmetric onsite discrete solitons for $\omega = 5$, $\gamma = 0.1$, and $\varepsilon = 1$. The right panel shows the imaginary-part of the spectrum as a function of the linear horizontal coupling parameter ε.

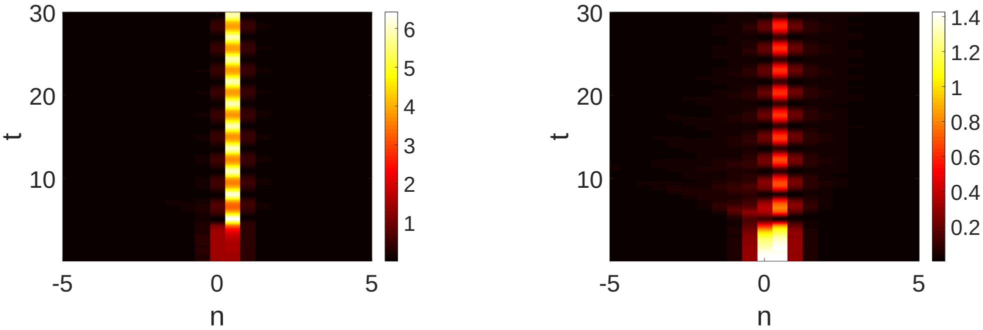

Fig. 7 The typical dynamics of unstable symmetric intersite discrete solitons with $\omega = 2$, $\gamma = 0.5$, $\varepsilon = 1$ (compare with Figure 1). The left and right panels depict the plots for $|u_n|^2$ and $|v_n|^2$, respectively.

intersite and onsite modes. Furthermore, each mode possesses three distinct configurations between the arms of the dimers, depending on the real-valued amplitudes of the time-independent solution of the model in the anticontinuum limit. These are symmetric, asymmetric, and antisymmetric structures.

We have also investigated the linear stability of the discrete soliton solutions by solving the corresponding linear eigenvalue problem. The continuous spectra lie on the imaginary axis and the parameter values determine the spectral boundaries. The corresponding discrete spectrum for the three structures of intersite discrete soliton admits one pair of eigenvalues bifurcating from the origin and two pairs of nonzero eigenvalues. On the other hand, for all three types of onsite discrete soliton, each structure possesses only one pair of nonzero discrete spectrum for small values of the horizontal linear coupling parameter.

We observed the dynamics of the discrete spectra ranging from the anticontinuum to continuum limits, which correspond to an increasing value of the horizontal linear coupling

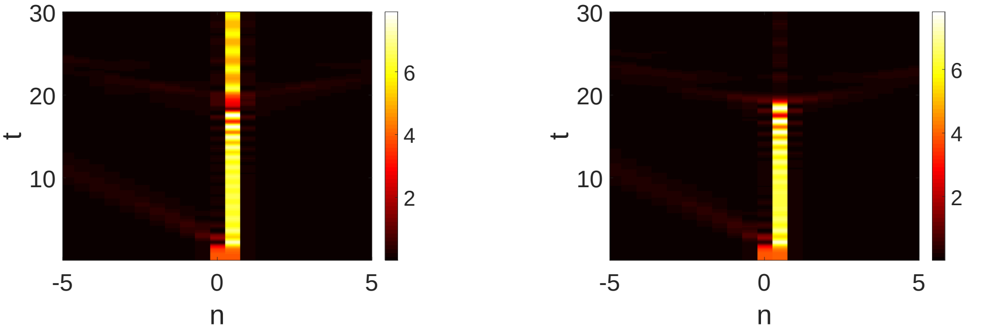

Fig. 8 Similar plots as Figure 7, they display the typical dynamics for an unstable antisymmetric intersite discrete soliton with the same parameter values (compare with Figure 2).

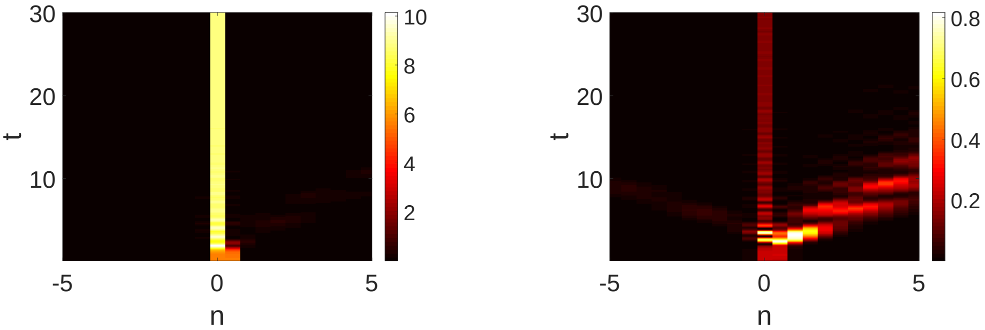

Fig. 9 Similar plots as Figure 7, they show the typical dynamics of unstable asymmetric intersite discrete solitons with $\omega = 5$, $\gamma = 0.5$, $\varepsilon = 1$ (compare with Figure 3).

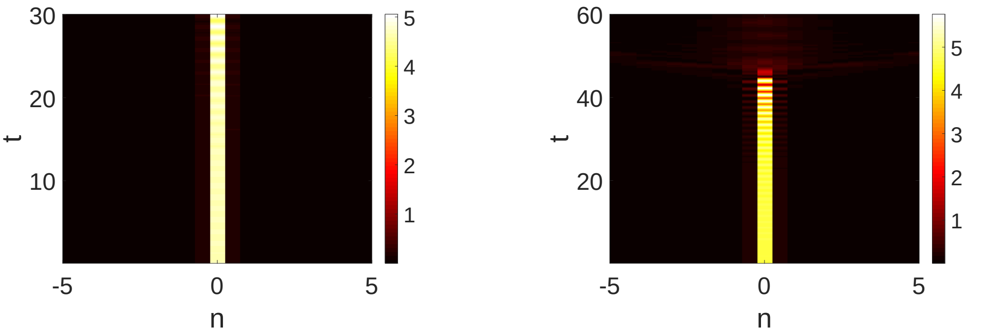

Fig. 10 Similar plots as Figure 7, they display the typical dynamics of unstable antisymmetric onsite discrete solitons with the same parameter values (compare with Figure 5).

parameter, for all the six types of discrete solitons. While all three types of intersite discrete solitons are always unstable, depending on the values of the propagation constant ω and the gain-loss parameter γ, onsite discrete solitons can be stable. A prevalent feature of the time dynamics for unstable discrete solitons is oscillation and annihilation as time progresses. For future research, in addition to extending the $\mathscr{PT}$-symmetric structure to a higher-dimensional model [57, 75], we can also implement a novel and universal method called the "bilinear neural network" for obtaining exact analytical solutions of the coupled DNLS equations [76].

Acknowledgements We are grateful to Professor Hadi Susanto, Department of Mathematical Sciences, University of Essex, UK and Department of Mathematics, Khalifa University, Abu Dhabi, The United Arab Emirates, for his assistance and valuable comments in improving this paper significantly.

Conflict of interest

The authors declare that they have no conflict of interest.

References

1. Bender, C.M., Boettcher, S.: Real spectra in non-Hermitian Hamiltonians having $\mathcal{PT}$ symmetry. Phys. Rev. Lett. **80**, 5243 (1998)
2. Bender, C.M., Boettcher, S., Meisinger, P.N.: $\mathcal{PT}$-symmetric quantum mechanics. J. Math. Phys. **40**(5), 2201 (1999)
3. Bender, C.M., Brody, D.C., Jones, H.F.: Complex extension of quantum mechanics. Phys. Rev. Lett. **89**, 270401 (2002)
4. Bender, C.M.: Making sense of non-Hermitian Hamiltonian. Rep. Prog. Phys. **70**, 947 (2007)
5. Moiseyev, N.: Non-Hermitian Quantum Mechanics. Cambridge University Press, Cambridge, UK, (2011)
6. Kottos, T.: Broken symmetry makes light work. Nat. Phys. **6**(3), 166 (2010)
7. Scott, D.D., Joglekar, Y.N.: Degrees and signatures of broken $\mathcal{PT}$ symmetry in nonuniform lattices. Phys. Rev. A **83**(5), 050102(R) (2011)
8. Pickton, J., Susanto, H.: Integrability of $\mathcal{PT}$-symmetric dimers. Phys. Rev. A **88**, 063840 (2013)
9. Burlak, G., Malomed, B.A.: Stability boundary and collisions of two-dimensional solitons in $\mathcal{PT}$-symmetric couplers with the cubic-quintic nonlinearity. Phys. Rev. E **88**(6), 062904 (2013)
10. Göksel, İ., Antar, N., Bakırtaç, İ: Solitons of $(1+1)$D cubic-quintic nonlinear Schrödinger equation with $\mathcal{PT}$-symmetric potentials. Optics Comm. **354**, 277 (2015)
11. Chen, Y.X.: Sech-type and Gaussian-type light bullet solutions to the generalized $(3+1)$-dimensional cubic-quintic Schrödinger equation in $\mathcal{PT}$-symmetric potentials. Nonlinear Dyn. **79**(1), 427 (2015)
12. Burlak, G., Garcia-Paredes, S., Malomed, B.A.: $\mathcal{PT}$-symmetric couplers with competing cubic-quintic nonlinearities. Chaos **26**(11), 113103 (2016)
13. Dai, C.Q., Chen, R.P., Wang, Y.Y., Fan, Y.: Dynamics of light bullets in inhomogeneous cubic-quintic-septimal nonlinear media with $\mathcal{PT}$-symmetric potentials. Nonlinear Dyn. **87**(3), 1675 (2017)
14. Li, P., Mihalache, D.: Symmetry breaking of solitons in $\mathcal{PT}$-symmetric potentials with competing cubic-quintic nonlinearity. Proc. Rom. Acad. A, **19**(1), 61 (2018)
15. Li, P., Dai, C., Li, R., Gao, Y.: Symmetric and asymmetric solitons supported by a $\mathcal{PT}$-symmetric potential with saturable nonlinearity: bifurcation, stability and dynamics. Opt. Express **26**(6), 6949 (2018)
16. Chen, S.J., Lin, J.N., Wang, Y.Y.: Soliton solutions and their stabilities of three $(2+1)$-dimensional $\mathcal{PT}$-symmetric nonlinear Schrödinger equations with higher-order diffraction and nonlinearities. Optik **194**, 162753 (2019)
17. Dong, L., Huang, C.: Double-hump solitons in fractional dimensions with a $\mathcal{PT}$–symmetric potential. Opt. Express **26**(8), 10509 (2018)
18. Yao, X., Liu, X.: Solitons in the fractional Schrödinger equation with parity-time-symmetric lattice potential. Photon. Res. **6**(9), 875 (2018)
19. Huang, C., Deng, H., Zhang, W., Ye, F., Dong, L.: Fundamental solitons in the nonlinear fractional Schrödinger equation with asymmetric potential. EPL (Europhys. Lett.) **122**(2), 24002 (2018)
20. Dong, L., Huang, C.: Vortex solitons in fractional systems with partially parity-time-symmetric azimuthal potentials. Nonlinear Dyn. **98**(2), 1019 (2019)
21. Li, F., Li, J., Han, B., Ma, H., Mihalache, D.: $\mathcal{PT}$-symmetric optical modes and spontaneous symmetry breaking in the space-fractional Schrödinger equation. Rom. Rep. Phys. **71**, 106 (2019)
22. Li, L., Li, H.G., Ruan, W., Leng, F.C., Luo, X.B.: Gap solitons in parity-time-symmetric lattices with fractional-order diffraction. JOSA B **37**(2), 488 (2020)
23. Solaimani, M.: Spectra of $\mathcal{PT}$-symmetric fractional Schrödinger equations with multiple quantum wells. J. Comput. Electron. 1 (2020)
24. Yan, Z.: Integrable $\mathcal{PT}$-symmetric local and nonlocal vector nonlinear Schrödinger equations: A unified two-parameter model. Appl. Math. Lett. **47**, 61 (2015)
25. Chen, H.Y., Zhu, H.P.: Self-similar azimuthons in strongly nonlocal nonlinear media with $\mathcal{PT}$-symmetry. Nonlinear Dyn. **84**(4), 2017 (2016)
26. Wen, Z., Yan, Z.: Solitons and their stability in the nonlocal nonlinear Schrödinger equation with $\mathcal{PT}$-symmetric potentials. Chaos **27**(5), 053105 (2017)
27. Xu, T., Li, H., Zhang, H., Li, M., Lan, S.: Darboux transformation and analytic solutions of the discrete $\mathcal{PT}$-symmetric nonlocal nonlinear Schrödinger equation. Appl. Math. Lett. **63**, 88 (2017)
28. Xu, T., Chen, Y., Li, M., Meng, D.X.: General stationary solutions of the nonlocal nonlinear Schrödinger equation and their relevance to the $\mathcal{PT}$-symmetric system. Chaos **29**(12), 123124 (2019)
29. Yang, B., Chen, Y.: Dynamics of rogue waves in the partially $\mathcal{PT}$-symmetric nonlocal Davey–Stewartson systems. Comm. Nonlinear Sci. Numer. Simulat. **69**, 287 (2019)
30. Rao, J., Cheng, Y., Porsezian, K., Mihalache, D., He, J.: $\mathcal{PT}$-symmetric nonlocal Davey–Stewartson I equation: soliton solutions with nonzero background. Physica D **401**, 132180 (2020).
31. Rao, J., He, J., Mihalache, D., Cheng, Y. $\mathcal{PT}$-symmetric nonlocal Davey–Stewartson I equation: General lump-soliton solutions on a background of periodic line waves. Appl. Math. Lett. **104**, 106246 (2020)
32. Yu, F., Li, L.: Dynamics of some novel breather solutions and rogue waves for the $\mathcal{PT}$-symmetric nonlocal soliton equations. Nonlinear Dyn. **95**(3), 1867 (2019)
33. Sun, B.: General soliton solutions to a nonlocal long-wave–short-wave resonance interaction equation with nonzero boundary condition. Nonlinear Dyn. **92**(3), 1369 (2018)
34. Deka, J.P., Sarma, A.K.: Chaotic dynamics and optical power saturation in parity–time ($\mathcal{PT}$) symmetric double-ring resonator. Nonlinear Dyn. **96**(1), 565 (2019)
35. Klauck, F., Teuber, L., Ornigotti, M., Heinrich, M., Scheel, S., Szameit, A.: Observation of $\mathcal{PT}$-symmetric quantum interference. Nat. Photon. **13** 1 (2019)
36. Deka, J.P., Sarma, A.K., Govindarajan, A., Kulkarni, M.: Multifaceted nonlinear dynamics in $\mathcal{PT}$-symmetric coupled Liénard oscillators. Nonlinear Dyn. **100**(2), 1629 (2020)
37. Jørgensen, M.F., Christiansen, P.L., Abou-Hayt, I.: On a modified discrete self-trapping dimer. Physica D **68**, 180 (1993)
38. Jørgensen, M.J., Christiansen, P.L.: Hamiltonian structure for a modified discrete self-trapping dimer. Chaos, Solitons & Fractals **4**, 217 (1994)
39. Gligorić, G., Radosavljević, A., Petrović, J., Maluckov, A., Hadžievski, L., Malomed, B.A.: Models of spin-orbit-coupled oligomers. Chaos **27**(11), 113102 (2017)
40. Guo, A., Salamo, G.J., Duchesne, D., Morandotti, R., Volatier-Ravat, M., Aimez, V., Siviloglou, G.A., Christodoulides, D.N.: Observation of $\mathcal{PT}$-symmetry breaking in complex optical potential. Phys. Rev. Lett. **103**, 093902 (2009)
41. Rüter, C.E., Makris, K.G., El-Ganainy, R., Christodoulides, D.N., Segev, M., Kip, D.: Observation of parity-time symmetry in optics. Nat. Phys. **6**, 192 (2010)
42. Ruschhaupt, A., Delgado, F., Muga, J.G.: Physical realization of $\mathcal{PT}$-symmetric potential scattering in a planar slab waveguide. J. Phys. A **38**, L171 (2005)
43. El-Ganainy, R., Makris, K.G., Christodoulides, D.N., Musslimani, Z.H.: Theory of coupled optical $\mathcal{PT}$-symmetric structures of coupled optical $\mathcal{PT}$-symmetric structures. Opt. Lett. **32**, 2632 (2007)
44. Klaiman, S., Günther, U., Moiseyev, N.: Visualization of branch points in $\mathcal{PT}$-symmetric waveguides. Phys. Rev. Lett. **101**, 080402 (2008)
45. Chen, Y., Snyder, A.W., Payne, D.N.: Twin core nonlinear couplers with gain and loss. Quantum Electronics **28**, 239 (1992)

46. Schindler, J., Li, A., Zheng, M.C., Ellis, F.M., Kottos, T.: Experimental study of active LRC circuits with $\mathscr{PT}$ symmetries. Phys. Rev. A **84**, 040101(R) (2011)
47. Ramezani, H., Schindler, J., Ellis, F.M., Günther, U., Kottos, T.: Bypassing the bandwidth theorem with $\mathscr{PT}$ symmetry. Phys. Rev. A **85**, 062122 (2012)
48. Lin, Z., Schindler, J., Ellis, F.M., Kottos, T.: Experimental observation of the dual behavior of $\mathscr{PT}$-symmetric scattering. Phys. Rev. A **85**, 050101(R) (2012)
49. Schindler, J., Lin, Z., Lee, J.M., Ramezani, H., Ellis, F.M., Kottos, T.: $\mathscr{PT}$-symmetric electronics. J. Phys. A: Math. Theor. **45**, 444029 (2012)
50. Bender, C.M., Gianfreda, M., Özdemir, Ş.K., Peng, B., Yang, L.: Twofold transition in $\mathscr{PT}$-symmetric coupled oscillators. Phys. Rev. A **88**, 062111 (2013)
51. Bender, C.M., Gianfreda, M., Klevansky, S.P.: Systems of coupled $\mathscr{PT}$-symmetric oscillators. Phys. Rev. A **90**, 022114 (2014)
52. Barashenkov, I.V., Gianfreda, M.: An exactly solvable $\mathscr{PT}$-symmetric dimer from a Hamiltonian system of nonlinear oscillators with gain and loss. J. Phys. A: Math. Theor. **47**, 282001 (2014)
53. Battelli, F., Diblík, J., Fečkan, M., Pickton, J., Pospíšil, M., Susanto, H.: Dynamics of generalized $\mathscr{PT}$-symmetric dimers with time-periodic gain-loss. Nonlinear Dyn. **81** 1 (2015)
54. Huang, C. Zeng, J.: Solitons stabilization in $\mathscr{PT}$ symmetric potentials through modulation the shape of imaginary component. Opt. Laser Technol. **88**, 104 (2017)
55. Barashenkov, I.V., Suchkov, S.V., Sukhorukov, A.A., Dmitriev, S.V., Kivshar, Y.S.: Breathers in $\mathscr{PT}$-symmetric optical couplers. Phys. Rev. A **86**(5), 053809 (2012)
56. Karthiga, S., Chandrasekar, V.K., Senthilvelan, M., Lakshmanan, M.: Systems that become $\mathscr{PT}$ symmetric through interaction. Phys. Rev. A **94**, 023829 (2016)
57. Chen, Y., Yan, Z., Mihalache, D., Malomed, B.A.: Families of stable solitons and excitations in the $\mathscr{PT}$-symmetric nonlinear Schrödinger equations with position-dependent effective masses. Sci. Rep. **7**(1), 1 (2017)
58. Jin, L., Zhang, X.Z., Zhang, G., Song, Z.: Reciprocal and unidirectional scattering of parity-time symmetric structures. Sci. Rep. **6**, 20976 (2016)
59. Jin L., Song, Z.: Incident direction independent wave propagation and unidirectional lasing. Phys. Rev. Lett. **121**, 073901 (2018)
60. Kevrekidis, P.G., Rasmussen, K.Ø., Bishop, A.R.: The discrete nonlinear Schrödinger equation: A survey of recent results. Int. J. Mod. Phys. B **15**(21), 2833 (2001)
61. Kivshar, Y.S., Agrawal, G.: Optical Solitons: From Fibers to Photonic Crystals. Fourth edition. Academic Press, Cambridge, Massachusetts (2003)
62. Kevrekidis, P.G.: The Discrete Nonlinear Schrödinger Equation. Mathematical Analysis, Numerical Computations, and Physical Perspectives. Vol. 232, Springer Science & Business Media, Berlin Heidelberg, Germany (2009).
63. Chernyavsky A., Pelinovsky, D.E.: Breathers in Hamiltonian $\mathscr{PT}$-symmetric chains of coupled pendula under a resonant periodic force. Symmetry **8**, 59 (2016)
64. Li, K., Kevrekidis, P.G., Susanto, H., Rothos, V.: Intrinsic localized modes in coupled DNLS equations from the anti-continuum limit. Math. Comp. Simul. **127**, 151 (2012)
65. Fan Z., Malomed, B.A.: Dynamical control of solitons in a parity-time-symmetric coupler by periodic management. Commun. Nonlinear Sci. Numer. Simulat. **79**, 104906 (2019)
66. Tombuloglu, S., Yuce, C.: Nonlinear waves in an anti-Hermitian lattice with cubic nonlinearity. Commun Nonlinear Sci. Numer. Simulat. **83**, 105106 (2020)
67. Kirikchi, O.B., Bachtiar, A.A., Susanto, H.: Bright solitons in a $\mathscr{PT}$-symmetric chain of dimers. Adv. Math. Phys. **2016**, 9514230 (2016)
68. Kirikchi, O.B., Malomed, B.A., Karjanto, N., Kusdiantara, R., Susanto, H.: Solitons in a chain of charge-parity-symmetric dimers. Phys. Rev. A **98**(6), 063841 (2018)
69. Susanto, H., Kusdiantara, R., Li, N., Kirikchi, O.B., Adzkiya, D., Putri, E.R.M., Asfihani, T.: Snakes and ghosts in a parity-time-symmetric chain of dimers. Phys. Rev. E **97**(6), 062204 (2018)
70. Xu, H., Kevrekidis, P.G., Saxena, A.: Generalized dimers and their Stokes-variable dynamics. J. Phys. A: Math. Theor. **48**, 055101 (2015)
71. Zeidler, E.: Applied Functional Analysis: Main Principles and Their Applications. Applied Mathematical Sciences Vol. 109, Springer-Verlag, New York, NY, USA (1995)
72. Accinelli, E.: A generalization of the Implicit Function Theorem. Appl. Math. Sci. **4**(26), 1289 (2010)
73. Alexeeva, N.V., Barashenkov, I.V., Rayanov, K., Flach, S.: Actively coupled optical waveguides. Phys. Rev. A **89**, 013848 (2014)
74. Dana, B., Bahabad, A., Malomed, B.A.: $\mathscr{CP}$ symmetry in optical systems. Phys. Rev. A **91**, 043808 (2015)
75. Muniz, A.L., Wimmer, M., Bisianov, A., Peschel, U., Morandotti, R., Jung, P.S., Christodoulides, D.N.: 2D solitons in $\mathscr{PT}$-symmetric photonic lattices. Phys. Rev. Lett. **123**(25), 253903 (2019)
76. Zhang, R.F., Bilige, S.: Bilinear neural network method to obtain the exact analytical solutions of nonlinear partial differential equations and its application to p-gBKP equation. Nonlinear Dyn. **95**(4), 3041 (2019)